Analyst

COMMUNICATION

View Article Online
View Journal | View Issue

Cite this: *Analyst*, 2017, **142**, 1054

Received 3rd October 2016,
Accepted 6th March 2017

DOI: 10.1039/c6an02221a

rsc.li/analyst

Raman spectroscopy compatible PDMS droplet microfluidic culture and analysis platform towards on-chip lipidomics†

Hyun Soo Kim,‡[a] Sergio C. Waqued,‡[b] Dawson T. Nodurft,[c] Timothy P. Devarenne,[d] Vladislav V. Yakovlev[b,c] and Arum Han*[a,b]

Lipids produced by microalgae are viewed as a potential renewable alternative to fossil fuels, however, significant improvements in productivity are required for microalgal biofuels to become economically feasible. Here we present a method that allows for the use of Raman spectroscopy with poly(dimethylsiloxane) (PDMS) droplet microfluidic devices, which not only overcomes the high Raman background of PDMS, but also achieves pairing of the high-throughput single-cell resolution advantages of droplet microfluidics with the direct, chemically specific, label-free, and non-destructive nature of Raman spectroscopy. The platform was successfully utilized for *in situ* characterization of microalgal lipid production over time within droplets, paving the way towards high-throughput microalgal lipidomics assays.

Introduction

Biofuel feedstock-producing microalgae have been heavily investigated as a renewable alternative to crude oil.[1–3] Microalgae convert light and CO_2 into a diverse range of lipids, from triacylglycerols (TAG) to long-chain hydrocarbons.[1] Lipids such as TAGs are generally produced when cells are stressed under adverse conditions such as nitrogen deprivation or photo-oxidation.[1] Current attempts to commercialize microalgal biofuels have only resulted in lipid yields that are estimated to be at least 10 to 20 times lower than that of the theoretical maximum, and thus are currently not economically feasible.[1,4] Further improvement in yield can be achieved through various ways, including developing better microalgal strains, optimizing culture conditions, and subsequently scaling up to large-scale cultures.[2,5,6] To reach these goals, extensive research in almost all aspects of microalgae is still needed, however, current microalgae culture systems such as open raceway ponds, closed photobioreactors, lab-scale flasks, and conventional multi-well culture plates lack high-throughput single-cell resolution screening capabilities, and thus are not suitable for many studies that require large numbers of testing to be conducted. New approaches overcoming these limitations can greatly accelerate and advance the current state of microalgal biofuel production.

Testing many different culture conditions in parallel can be increased by several orders of magnitude over existing flask or multi-well plate experimentation when utilizing droplet microfluidics, where pico- or nano-liter scale water-in-oil emulsion droplets are used as miniature isolated bioreactor or culture vessels.[7–10] These systems use carrier oil to section small volumes of water-based fluids such as cell-containing culture media into droplets, each encapsulating one or more cells. These droplets can be individually transported, mixed, merged, split, and analyzed, which allows for complex biological assays to be conducted with single-cell resolution at extremely high-throughput.[7–10] Thus, droplet microfluidics-based systems have emerged as a powerful tool for broad ranges of biological assays requiring high-throughput assays, and have started to be utilized in microalgal biofuel developments, including various screening applications to identify microalgal strains showing enhanced growth and/or lipid production and to quickly optimize culture conditions that results in improved productivity.[10–12]

In any of these efforts, the lipid content, both in terms of quantity and lipid type, needs to be continuously or periodically measured throughout the culturing process. Lipid analysis methods typically used in droplet microfluidics rely on optical detection of fluorescent markers. Lipophilic fluorescent dyes such as Nile red or BODIPY is commonly used and convenient, however, these dyes only allow for single time-

[a]*Department of Electrical and Computer Engineering, Texas A&M University, College Station, Texas, USA. E-mail: arum.han@ece.tamu.edu; Tel: +1 979 845 9686 or +1 979 318 2430*
[b]*Department of Biomedical Engineering, Texas A&M University, College Station, Texas, USA*
[c]*Department of Physics and Astronomy, Texas A&M University, College Station, Texas, USA*
[d]*Department of Biochemistry and Biophysics, Texas A&M University, College Station, Texas, USA*

†Electronic supplementary information (ESI) available. See DOI: 10.1039/c6an02221a

‡These authors contributed equally to this work.

point lipid analysis as they photobleach quickly over time and also cause cytotoxicity due to chemicals (*e.g.*, dimethyl sulfoxide (DMSO)) in which the dyes have to be dissolved, making time-course analysis challenging or impossible.[13] Additionally, fluorescent dyes can only provide information regarding total lipid amount as these dyes indiscriminately stain all neutral lipids,[13] thus significantly limiting the on-chip lipid analysis capability. Destructive analysis techniques commonly used in conventional cultures such as solvent extraction and subsequent chromatography (HPLC or GC),[14] NMR,[15] or mass spectrometry,[16] are capable of examining both quantification and identification of lipid types, but cannot be applied to droplet microfluidics, mainly due to the large sample amounts required for analysis, which is very challenging to realize in micro-scale devices that handle very small volumes. In addition, the destructive nature of these assays are not compatible with single-cell resolution analysis where the target cells to be analyzed have to be also preserved.

Recently, Raman spectroscopy has emerged as an alternative method for microalgal lipid analysis, which provides both chemical identification and quantification without the need for molecular tagging or destroying cell samples.[16–18] The Raman spectrum is unique to a given set of molecular bonds, thus providing chemical specificity for lipid analyses, and the spectrum peak intensities can be used to quantify each lipid component as they correlate with the number of molecules in the focal volume.[19–22] Therefore, Raman spectroscopy is a promising tool for label-free and non-destructive lipidomics with single-cell resolution. The pairing of high-throughput droplet microfluidic platforms with Raman spectroscopic analysis[23–28] will allow for rapid quantification and identification of *in vivo* lipid production at the single-cell level without necessitating any downstream destructive processing. However, there are two barriers to overcome for achieving this integration. First, poly(dimethylsiloxane) (PDMS) is the primary material of choice used for microfluidic cell culture devices, specifically due to its excellent gas permeability that is necessary for successful multi-day microalgal culture, and its optical transparency, which allows for the provision of light for photosynthesis as well as optical monitoring of the cell culture.[29] In addition, PDMS devices are easy to microfabricate, and thus droplet microfluidic systems have almost exclusively been fabricated in PDMS. However, PDMS generates an extremely strong Raman scattering signal,[30] which overwhelms the relatively weak signal from single cells. Second, the carrier oil needed in droplet microfluidics can mask the Raman signal of the microalgal lipids to be analyzed within the droplets.[31]

Herein, we describe a method that allows for the use of Raman spectroscopy with PDMS-based microdevices to perform on-chip, droplet-based *in vivo* biomolecular analysis (*i.e.*, microalgal lipid analysis) with single-cell resolution. The system was characterized and demonstrated by conducting on-chip Raman spectroscopic analysis of lipid accumulation in the microalgae *Chlamydomonas reinhardtii* and *Botryococcus braunii* in the droplet microfluidic systems. Particularly, the ability of the system was validated through time-course tracking and analysis of differential lipid accumulation in *C. reinhardtii* cells under 8 different culture conditions.

Materials and methods

Design and fabrication of microfluidic devices

The microfluidic device (height: 100 μm) consists of a traditional T-junction droplet generator[9,10] that is placed directly upstream of an array of eight large droplet culture chambers (Fig. 1). The droplet generator is composed of two crossing channels, a 200 μm wide channel for carrier oil flow and a perpendicular 160 μm wide channel for cell solution flow. Each downstream culture chamber has a volume of 10 μl in which approximately 1000 droplets can be stored, cultured, and examined over time. Eight culture chambers in the microdevice allows for 8 different culture conditions to be tested in parallel on a single chip for examining microalgal lipid production under the given culture conditions.

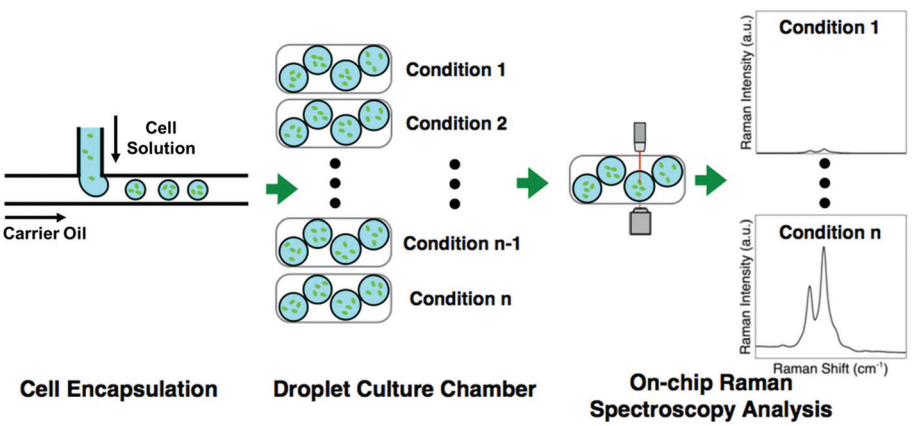

Fig. 1 Overview of Raman spectroscopy integrated with a PDMS droplet microfluidic platform for on-chip droplet formation, culture, and *in vivo* cellular lipid analysis.

The device was fabricated in PDMS (Sylgard® 184 Dow Corning, Inc., Midland, MI) using the soft-lithography method as previously described.[9,10] After PDMS device replication (layer thickness: 4 mm), the droplet generator and culture chamber layer was bonded to a 24 × 60 mm^2 cover glass slide (VWR, West Chester, PA). The thin cover glass was chosen as the device substrate to further decrease spectral background originating from the device materials. The assembled device was pre-treated with Aquapel (Pittsburg Glass Works, LLC) to improve channel surface hydrophobicity for consistent droplet generation and also to minimize device-to-droplet wetting interactions.[32] After the coating, each channel was dried using nitrogen gas and subsequently filled with Fluorinert Electronic Liquid FC-40 (3M), which was used as the carrier oil.

Preparation of *Botryococcus braunii* and *Chlamydomonas reinhardtii*

The colony-forming green microalga *Botryococcus braunii* race B, Showa (or Berkeley) strain[33] (single cell size: 13 μm × 7–9 μm), and the unicellular microalga *Chlamydomonas reinhardtii*, CC-4333 (cw15 arg707 sta6-1) strain (single cell size: 5–10 μm), were cultured in standard Chu-13 [34] and tris-acetate-phosphate (TAP) medium[35] (100% nitrogen), respectively, under a 13W compact fluorescent (65K) light that generates an irradiance of 80 μmol photons per m^2 per s. The cultures underwent a 12-hour light–dark cycle for 7 days before being loaded onto the microdevices for Raman spectroscopic lipid analysis. For time-course tracking of lipid accumulation under different culture conditions, *C. reinhardtii* cells were diluted (concentration: 1.65 × 10^6 cells per mL) and resuspended in TAP medium having 8 different nitrogen concentrations (0, 15, 30, 45, 60, 75, 90, and 100% nitrogen) prior to on-chip droplet encapsulation and culture. Centrifugation and resuspension was repeated at least three times to ensure complete change-over to the new medium.

Cell encapsulation

Water-in-oil emulsion droplets (diameter: 250 μm) that contained 10–15 cells were generated by flowing a cell solution and FC-40 carrier oil having 1% 008-FluoroSurfactant (RAN Biotechnologies) at flow rates of 300 μL h^{-1} and 500 μL h^{-1}, respectively, into the T-junction device. Once the droplets moved into and completely filled the downstream culture chamber, the inlet and outlet tubings were clamped to seal droplets in the chamber. After droplet encapsulation, the microdevices were maintained in a humidified environment throughout the experiments to prevent droplet evaporation through the gas-permeable PDMS layer.[12]

Raman spectroscopy

Raman spectra were collected using a confocal Raman microscope (Horiba LabRAM HR Evolution, Jobin–Yvon). A 50× objective (NA: 0.75) was used for focusing a 532 nm wavelength laser (spot size: approximately 1.5 μm) onto single cells and for collecting Raman scattered light, which was then dispersed by a 1800 lines per millimeter grating. The 532 nm laser was chosen compared to 660 nm and 785 nm excitation, as this excitation acquired higher signal-to-noise ratio Raman spectra and also provided faster bleaching of background chlorophyll autofluorescence. The acquisition time was fixed to 20 seconds with two accumulations for each collection window. To determine confocal reduction of PDMS background spectra, 200 μm (= 4.6 Airy units) and 25 μm (= 0.58 Airy units) pinholes were used and the results were compared. The laser was manually aimed at single cells and spectral data were only retained if the cell was still in the same location after all spectra have been collected.

Time-course analysis of microalgal lipid production

The Raman spectral peak at 1657 cm^{-1} (C═C stretching) has been shown to be specific for fatty acid *cis* C═C bonds,[36–39] and thus selected as a reference peak to measure microalgal lipid (TAG) accumulation under 8 different nitrogen concentration conditions. The peak intensity was collected and averaged from 10 different droplets every 24 hours for each culture condition. For comparison with conventional fluorescent tagging based lipid analysis, *C. reinhardtii* cells grown under 8 different nitrogen concentrations were also stained with Nile red, a fluorescent lipophilic dye previously shown to stain microalgal lipids,[10,13,40–42] every 24 hours. After staining, microscopic images of chlorophyll autofluorescence and Nile red fluorescence were taken using a Zeiss Axio Observer Z1 microscope equipped with a Hamamatsu ORCA-Flash2.8 CMOS camera (excitation: 450–490 nm, emission for chlorophyll >610 nm, emission for Nile red: 560–600 nm). To quantify lipid production per unit cell volume, the Nile red fluorescence intensity sum was divided by the chlorophyll autofluorescence intensity sum, and then averaged over 5 cells for each nitrogen culture condition. The Raman peak intensity and Nile red staining results were then correlated to each time point and culture conditions for comparison.

Results and discussion

Raman spectra background reduction

The Raman spectra of the microalga *Botryococcus braunii* inside PDMS devices were collected in both a standard upright orientation and an inverted orientation to compare the effect of PDMS thickness on the Raman background signal. Similar to previously reported studies,[26,43] inversion of the PDMS microfluidic culture device drastically reduced the Raman scattered light from PDMS, thereby allowing for *in vivo* microalgal lipid spectra to be accurately acquired (ESI and Fig. S1†). The inverted microfluidic device containing *B. braunii* was then used to investigate the confocal reduction of background spectra resulting from out of focus materials. A large confocal pinhole diameter (4.6 AU) was chosen to obtain the spectra without confocal sectioning (Fig. 2A). Raman peaks derived from lipids were detectable in the spectra at 1440 cm^{-1} and

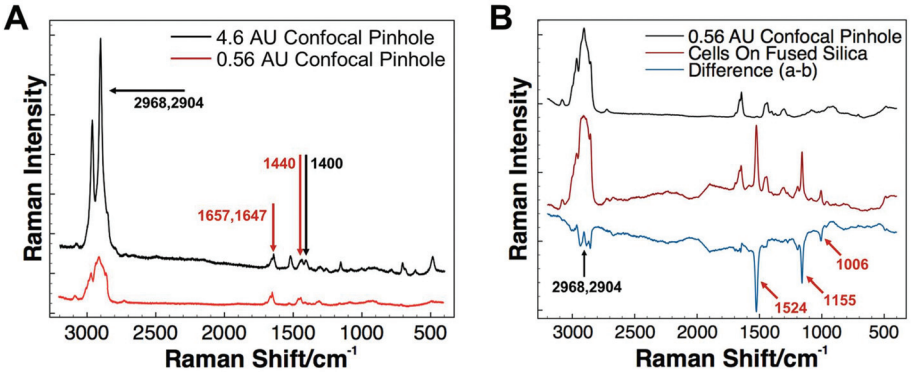

Fig. 2 Adjusting confocal pinhole size to further reduce PDMS Raman background. (A) Comparison of Raman spectra of *B. braunii* using 4.6 (black) and 0.56 (red) Airy unit confocal pinholes. Peaks resulting from PDMS are marked with black arrows, whereas red arrows indicate peaks resulting from lipids. (B) Raman spectra of *B. braunii* when using a 0.56 Airy unit confocal pinhole (black), *B. braunii* on a fused silica substrate (red), and the difference of the two spectra (blue). Peaks resulting from PDMS are marked with a black arrow, whereas red arrows indicate peaks resulting from carotenoids.

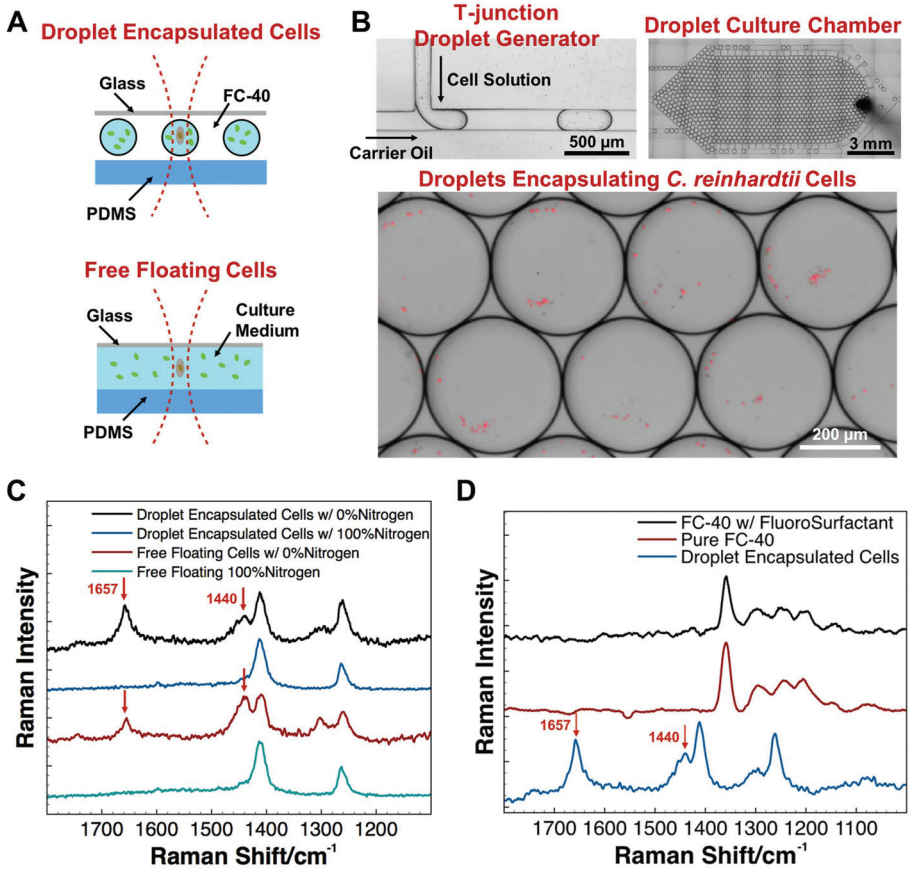

Fig. 3 Comparison of spectra from free-floating and droplet-encapsulated *C. reinhardtii* cells. (A) Illustration showing the confocal focusing of cells (highlighted in red) encapsulated in a droplet (top) and floating freely in a PDMS channel (bottom). (B) Microscopic images showing droplet generation through the T-junction droplet generator, the culture chamber filled with droplets, and an enlarged view of droplets inside the culture chamber, which contain 10–15 *C. reinhardtii* cells as visualized by chlorophyll autofluorescence colored in red. (C) Raman spectra of *C. reinhardtii* cells encapsulated in a droplet (black; 0% nitrogen, blue; 100% nitrogen) and free floating in culture media within a PDMS channel (red; 0% nitrogen, green; 100% nitrogen). (D) Background spectra of FC-40 carrier oil compared to *C. reinhardtii* spectra. Peaks resulting from FC-40 with FluoroSurfactant (black) and pure FC-40 (red) are not observed in the microalgal spectra (blue). Lipid peaks are marked with red arrows.

1657 cm^{-1} (CH_2 bending and C=C stretching, respectively),[37] however the strong PDMS scattering overwhelmed much of the spectra (Fig. 2A). By reducing the confocal pinhole size by a factor of eight, the Airy unit parameter was brought down close to one-eighth, which greatly reduced the out of focus background to almost negligible levels (Fig. 2A).

For ease of comparison, the spectra of cells in the inverted device were subtracted from that of cells on a fused silica (quartz) substrate (Fig. 2B). The background from the glass coverslip is shown to be roughly equivalent to that of the fused silica. The major spectral differences between the two samples result from a weak PDMS signal at 2968 cm^{-1} and 2904 cm^{-1} as well as three strong peaks assigned to carotenoids at 1524 cm^{-1}, 1155 cm^{-1}, and 1006 cm^{-1} (Fig. 2B).[37,39] The sandwiching of the sample between the silica slide and coverslip squeezed *B. braunii* colonies, where a 3D colonial shape spread into a 2D-like planar structure, allowing for more precise examination (*i.e.*, carotenoid detection).[10] The lipid spectra in the on-chip microalgal cells can be clearly visualized *in situ* with little impact from background Raman scattering coming from the device material itself, and were comparable to traditional microscope slide based Raman spectroscopic analysis.

Compatibility with droplet microfluidic systems

Droplet-based microfluidic devices can provide extremely high-throughput operations, and thus have broad applicability in microalgal biofuel development. To determine whether on-chip Raman analysis of microalgal lipids is also possible and compatible with droplet microfluidic systems made out of PDMS, non-motile *C. reinhardtii* cells were prepared both in droplet format and free-floating in a microfluidic channel (Fig. 3A and B). The spectra for cells in both conditions were collected and compared to determine if the fluorinated carrier oil FC-40 would introduce any background peaks to the lipid spectra (Fig. 3C). As can be seen, there were no additional peaks observed in both cases (Fig. 3C), and therefore the differences in peak intensities between cells accumulating lipids (cultured in 0% nitrogen medium) and those without lipids (cultured in 100% nitrogen medium) can be attributed to different intracellular lipid concentrations. To further investigate the potential background contributions of the FC-40 carrier oil, the Raman spectra was collected for the oil itself with and without the dissolved FluoroSurfactant (Fig. 3D). The FC-40 carrier oil spectra with and without FluoroSurfactant were shown to not contain any additional peaks within the region of interest between 1800 cm^{-1} and 1400 cm^{-1} (Fig. 3D).

Time-course analysis of *C. reinhardtii* lipid production under different in-droplet culture conditions

C. reinhardtii cells are known to produce TAG lipids under stressed conditions such as nitrogen deprivation, and the accumulated amount of lipid is also known to be dependent on the level of stress applied.[10] Droplets containing *C. reinhardtii* cells under 8 different culture conditions (0, 15, 30, 45, 60, 75, 90, and 100% nitrogen in TAP medium) were prepared and cultured on-chip to investigate and compare the effects of different amounts of nitrogen in culture media on microalgal lipid production. The C=C stretch Raman scattering peak at 1657 cm^{-1} was chosen as the indicator of cellular fatty acid lipids in the form of TAGs (Fig. 3D) and used to track lipid production by cells cultured under the 8 different culture conditions over 4 days. Droplets stored in the culture chamber were stable, where no droplet merging or evaporation were observed during the entire culture period. In this analysis, Raman spectroscopic measurement across multiple time points without any preparation steps allowed for quantification of daily lipid changes in the same *C. reinhardtii* cells over time. The results show that cells under the stressed low-nitrogen conditions accumulated the most amount of lipids (Fig. 4A). In addition, the level of lipid accumulation at the final time point corresponded well with the level of nitrogen depletion (Fig. 4A).

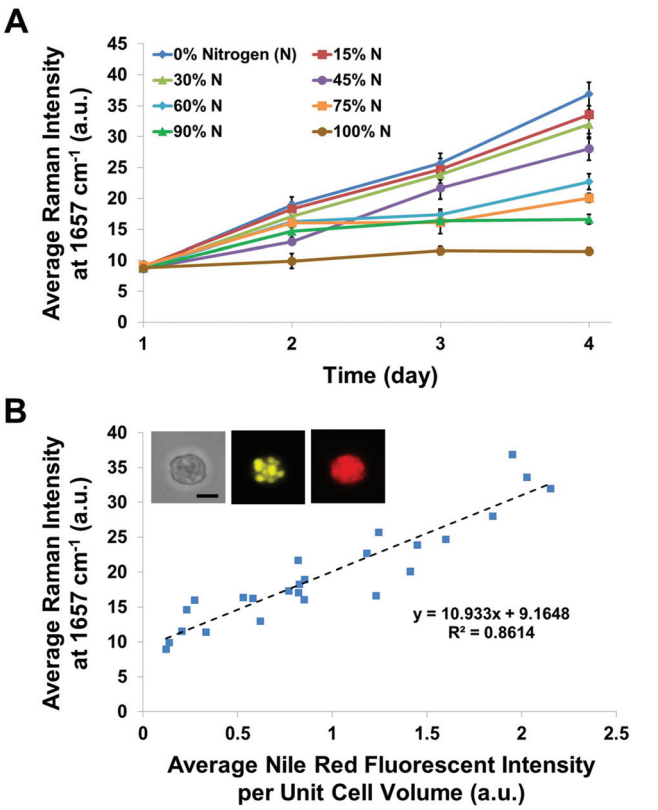

Fig. 4 Time-course Raman spectroscopic analysis of lipid production in *C. reinhardtii* under 8 different nitrogen concentration culture conditions. (A) Average Raman peak intensity of *C. reinhardtii* cells inside droplets at 1657 cm^{-1}, analyzed for 4 days under 8 different nitrogen concentrations (n = 10). All data shown are mean ± standard error. (B) Correlation between average Raman peak intensity at 1657 cm^{-1} and average Nile red fluorescence intensity per unit cell volume (fluorescence intensity of Nile red stained lipid divided by chlorophyll autofluorescence intensity) in *C. reinhardtii* cells for all measured culture conditions (R^2 = 0.8614). Inset shows an example of a Nile red stained *C. reinhardtii* cell (yellow; stained oil bodies) cultured in 0% nitrogen condition for 3 days. Red color indicates chlorophyll autofluorescence. Scale bar = 5 μm.

To compare the Raman spectroscopic analysis with conventional fluorescent dye based analysis, the Raman intensities obtained from the time-course measurements were compared to the Nile red staining results (Fig. 4B). The two quantification methods showed a strong correlation (R^2 = 0.8614; Fig. 4B), indicating that the on-chip Raman spectra can be used to quantify the amount of intracellular lipids produced by cells without the need for any invasive fluorescent staining.

Conclusion

Here we present a method that allows for the use of Raman spectroscopy with droplet microfluidic devices made with PDMS, where the PDMS Raman spectral background was minimized through the use of a confocal pinhole and inverse device orientation. Using two different microalgal cells, we demonstrated the compatibility of droplet microfluidic systems that utilize oil as the carrier liquid for the water-in-oil emulsion droplets with Raman spectroscopy for microalgal lipid analysis. We then used a droplet microfluidic culture platform having 8 different droplet culture chambers and successfully demonstrated the ability for *in vivo* analysis of lipid production from both colony-forming and unicellular microalgal strains, including demonstration of the effect of nitrogen depletion on lipid production in both free-floating culture and droplet-culture formats. These findings will allow for the pairing of Raman spectroscopy with droplet microfluidics based microalgal culture/screening assays to enable label-free, real-time, non-destructive, single-cell resolution lipid analysis for the development of next-generation microalgal biofuels. Furthermore, we expect that the application of such a platform could be expanded to real-time investigation of any intracellular processes in microfluidic cell culture platforms using Raman spectroscopy, particularly those benefitting from increased parallelization and high-throughput features of droplet microfluidics.

Acknowledgements

This work was supported by the National Science Foundation (NSF) Emerging Frontiers in Research and Innovation (EFRI) grant #1240478 to A. H. and T. P. D., the NSF DBI grant #1532188 to A. H. and V. V. Y., and the NSF grant #HRD-1249272 to S. C. W. Any opinions, findings, and conclusions or recommendations expressed in this material are those of the author(s) and do not necessarily reflect the views of the NSF.

References

1 Q. Hu, M. Sommerfeld, E. Jarvis, M. Ghirardi, M. Posewitz, M. Seibert and A. Darzins, *Plant J.*, 2008, **54**, 621–639.
2 L. Rodolfi, G. Chini Zittelli, N. Bassi, G. Padovani, N. Biondi, G. Bonini and M. R. Tredici, *Biotechnol. Bioeng.*, 2009, **102**, 100–112.
3 A. Han, H. Hou, L. Li, H. S. Kim and P. de Figueiredo, *Trends Biotechnol.*, 2013, **31**, 225–232.
4 Y. Ma, Z. Wang, M. Zhu, C. Yu, Y. Cao, D. Zhang and G. Zhou, *Bioresour. Technol.*, 2013, **136**, 360–367.
5 Y. Chisti, *J. Biotechnol.*, 2013, **167**, 201–214.
6 D. R. Georgianna and S. P. Mayfield, *Nature*, 2012, **488**, 329–335.
7 A. Rakszewska, J. Tel, V. Chokkalingam and W. T. S. Huck, *NPG Asia Mater.*, 2014, **6**, e133.
8 D. Hummer, F. Kurth, N. Naredi-Rainer and P. S. Dittrich, *Lab Chip*, 2016, **16**, 447–458.
9 A. R. Guzman, H. S. Kim, P. de Figueiredo and A. Han, *Biomed. Microdevices*, 2015, **17**, 35.
10 H. S. Kim, A. R. Guzman, H. R. Thapa, T. P. Devarenne and A. Han, *Biotechnol. Bioeng.*, 2016, **113**, 1691–1701.
11 Y. J. Sung, J. Y. Kim, K. W. Bong and S. J. Sim, *Analyst*, 2016, **141**, 989–998.
12 A. Dewan, J. Kim, R. H. McLean, S. A. Vanapalli and M. N. Karim, *Biotechnol. Bioeng.*, 2012, **109**, 2987–2996.
13 J. Rumin, H. Bonnefond, B. Saint-Jean, C. Rouxel, A. Sciandra, O. Bernard, J. P. Cadoret and G. Bougaran, *Biotechnol. Biofuels*, 2015, **8**, 42.
14 V. H. Work, R. Radakovits, R. E. Jinkerson, J. E. Meuser, L. G. Elliott, D. J. Vinyard, L. M. Laurens, G. C. Dismukes and M. C. Posewitz, *Eukaryotic Cell*, 2010, **9**, 1251–1261.
15 J. S. Craigie, S. L. MacKinnon and J. A. Walter, *J. Appl. Phycol.*, 2007, **20**, 665–671.
16 T. L. Weiss, H. J. Chun, S. Okada, S. Vitha, A. Holzenburg, J. Laane and T. P. Devarenne, *J. Biol. Chem.*, 2010, **285**, 32458–32466.
17 O. Samek, P. Zemánek, A. Jonáš and H. H. Telle, *Laser Phys. Lett.*, 2011, **8**, 701–709.
18 S. R. Fagerer, T. Schmid, A. J. Ibanez, M. Pabst, R. Steinhoff, K. Jefimovs, P. L. Urban and R. Zenobi, *Analyst*, 2013, **138**, 6732–6736.
19 B. L. Milman, *TrAC, Trends Anal. Chem.*, 2005, **24**, 493–508.
20 J. R. Mourant, J. Dominguez, S. Carpenter, K. W. Short, T. M. Powers, R. Michalczyk, N. Kunapareddy, A. Guerra and J. P. Freyer, *J. Biomed. Opt.*, 2006, **11**, 064024.
21 J. P. Day, K. F. Domke, G. Rago, H. Kano, H. O. Hamaguchi, E. M. Vartiainen and M. Bonn, *J. Phys. Chem. B*, 2011, **115**, 7713–7725.
22 K. Czamara, K. Majzner, M. Z. Pacia, K. Kochan, A. Kaczor and M. Baranska, *J. Raman Spectrosc.*, 2015, **46**, 4–20.
23 S. E. Barnes, Z. T. Cygan, J. K. Yates, K. L. Beers and E. J. Amis, *Analyst*, 2006, **131**, 1027–1033.
24 P. C. Ashok, G. P. Singh, H. A. Rendall, T. F. Krauss and K. Dholakia, *Lab Chip*, 2011, **11**, 1262–1270.
25 Z. Pilát, J. Ježek, J. Kaňka and P. Zemánek, *Proc. SPIE*, 2014, **8947**, 89471M–89479M.

26 B. M. Liszka, H. S. Rho, Y. Yang, A. T. M. Lenferink, L. W. M. M. Terstappen and C. Otto, *RSC Adv.*, 2015, **5**, 49350–49355.
27 A. Marz, T. Henkel, D. Cialla, M. Schmitt and J. Popp, *Lab Chip*, 2011, **11**, 3584–3592.
28 P. Zhang, L. Ren, X. Zhang, Y. Shan, Y. Wang, Y. Ji, H. Yin, W. E. Huang, J. Xu and B. Ma, *Anal. Chem.*, 2015, **87**, 2282–2289.
29 T. Merkel, V. Bondar, K. Nagai, B. Freeman and I. Pinnau, *J. Polym. Sci., Part B: Polym. Phys.*, 2000, **38**, 415–434.
30 F. Sarrazin, J.-B. Salmon, D. Talaga and L. Servant, *Anal. Chem.*, 2008, **80**, 1689–1695.
31 E. C. Santos, H. S. Martinho, K. Annes, R. F. Leite and M. P. Milazzotto, *Biomed. Opt. Express*, 2015, **6**, 2830–2839.
32 L. Mazutis, J. Gilbert, W. L. Ung, D. A. Weitz, A. D. Griffiths and J. A. Heyman, *Nat. Protoc.*, 2013, **8**, 870–891.
33 A. M. Nonomura, *Jpn. J. Phycol.*, 1988, **36**, 285–291.
34 M. Grung, P. Metzger and S. Liaaen-jensen, *Biochem. Syst. Ecol.*, 1989, **17**, 263–269.
35 D. S. Gorman and R. P. Levine, *Proc. Natl. Acad. Sci. U. S. A.*, 1965, **54**, 1665–1669.
36 G. F. Bailey and R. J. Horvat, *J. Am. Oil Chem. Soc.*, 1972, **49**, 494–498.
37 H. Wu, J. V. Volponi, A. E. Oliver, A. N. Parikh, B. A. Simmons and S. Singh, *Proc. Natl. Acad. Sci. U. S. A.*, 2011, **108**, 3809–3814.
38 X. He, J. Allen, P. Black, T. Baldacchini, X. Huang, H. Huang, L. Jiang and Y. Lu, *Biomed. Opt. Express*, 2012, **3**, 2896–2906.
39 O. Samek, A. Jonas, Z. Pilat, P. Zemanek, L. Nedbal, J. Triska, P. Kotas and M. Trtilek, *Sensors*, 2010, **10**, 8635–8651.
40 K. E. Cooksey, J. B. Guckert, S. A. Williams and P. R. Callis, *J. Microbiol. Methods*, 1987, **6**, 333–345.
41 H. S. Kim, T. P. Devarenne and A. Han, *Lab Chip*, 2015, **15**, 2467–2475.
42 H. S. Kim, T. L. Weiss, H. R. Thapa, T. P. Devarenne and A. Han, *Lab Chip*, 2014, **14**, 1415–1425.
43 Y. Geng, L. Chen, G. Chen, W. Bi, S. Xu, H. Cui and W. Xu, *Rev. Sci. Instrum.*, 2015, **86**, 056109.